AD-A107 041 NAVAL RESEARCH LAB WASHINGTON DC F/G 12/1
HIGH SOLITARY WAVES IN WATER: A REFINED NUMERICAL METHOD.(U)
SEP 81 J M WITTING, J M BERGIN
UNCLASSIFIED NRL-8504 NL

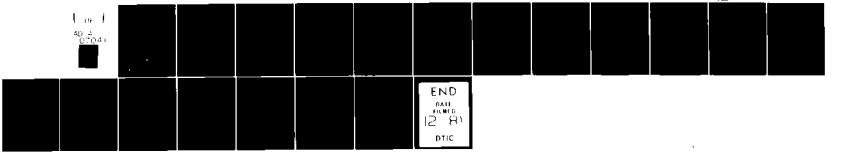

(2) LEVEL II

NRL Report 8504

AD A107041

High Solitary Waves in Water: A Refined Numerical Method

JAMES M. WITTING AND JOHN M. BERGIN

Physical Oceanography Branch
Environmental Sciences Division

September 30, 1981

NAVAL RESEARCH LABORATORY
Washington, D.C.

SECURITY CLASSIFICATION OF THIS PAGE (When Data Entered)

REPORT DOCUMENTATION PAGE

READ INSTRUCTIONS BEFORE COMPLETING FORM

1 REPORT NUMBER: NRL 8504	2 GOVT ACCESSION NO.
3 RECIPIENT'S CATALOG NUMBER	
4 TITLE (and Subtitle): HIGH SOLITARY WAVES IN WATER: A REFINED NUMERICAL METHOD	5 TYPE OF REPORT & PERIOD COVERED: Interim report on a continuing NRL problem
6 PERFORMING ORG. REPORT NUMBER	
7 AUTHOR(s): James M. Witting and John M. Bergin	8 CONTRACT OR GRANT NUMBER(s)
9 PERFORMING ORGANIZATION NAME AND ADDRESS: Naval Research Laboratory, Washington, D.C. 20375	10 PROGRAM ELEMENT, PROJECT, TASK AREA & WORK UNIT NUMBERS: 43-1140-0-1
11 CONTROLLING OFFICE NAME AND ADDRESS	12 REPORT DATE: September 30, 1981
	13 NUMBER OF PAGES: 18
14 MONITORING AGENCY NAME & ADDRESS (if different from Controlling Office)	15 SECURITY CLASS. (of this report): UNCLASSIFIED
	15a DECLASSIFICATION/DOWNGRADING SCHEDULE

16 DISTRIBUTION STATEMENT (of this Report)

Approved for public release; distribution unlimited.

17 DISTRIBUTION STATEMENT (of the abstract entered in Block 20, if different from Report)

18 SUPPLEMENTARY NOTES

19 KEY WORDS (Continue on reverse side if necessary and identify by block number)

Solitary waves
Water wave
Numerical methods
Applied mathematics
Physical oceanography

20 ABSTRACT (Continue on reverse side if necessary and identify by block number)

Formerly, finite difference calculations of solitary wave properties gave results different from those obtained from independent methods. Calculations based on an expansion in powers of a small quantity, supplemented by the use of Padé approximates, and calculations based on an integral equation for the wave profile are in satisfactory agreement, except possibly for the highest waves. This report refines and extends a numerical method based on Fourier series solutions of the governing equations. The resultant solitary wave properties agree with those found by independent methods to several significant figures, except for waves having amplitudes within a few percent of

(Continues)

DD FORM 1 JAN 73 1473 EDITION OF 1 NOV 65 IS OBSOLETE
S/N 0102-014-6601

SECURITY CLASSIFICATION OF THIS PAGE (When Data Entered)

20 ABSTRACT (Continued)

that of the highest wave. There appears to be little degradation in the method's accuracy for the highest and very high waves, when compared to waves of intermediate height. This report discusses possible reasons for the failure of other numerical work to achieve high accuracy.

CONTENTS

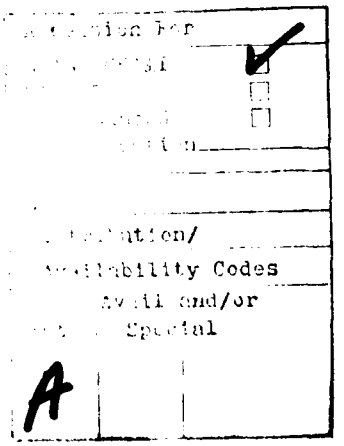

HIGH SOLITARY WAVES IN WATER: A REFINED NUMERICAL METHOD

1. INTRODUCTION

This report describes a numerical method for analyzing the properties of solitary waves in water and assesses the method's accuracy. A second report (J. M. Witting, "High Solitary Waves in Water: Results of Calculations," NRL Report 8505) presents detailed and comprehensive results.

Figure 1 presents the motivation for the research and hints at some of the results. The figure plots the square of the speed of a solitary wave in water against its amplitude. The plot is nondimensional; speeds are referenced to the speed of long linear waves in water; amplitudes are referenced to the water depth well away from the solitary wave. To make the figure legible, only high solitary waves are shown. The complete curve would extend downward to a speed of unity and an amplitude of zero. It terminates with the highest wave in water. The highest wave has a "kineticity" twice the amplitude.* Figure 1 shows the limiting relationship as a barrier.

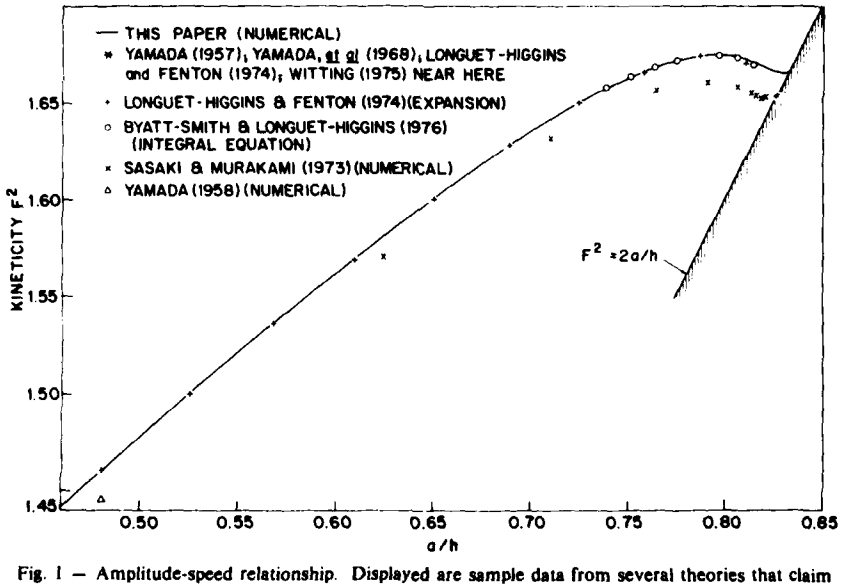

Fig. 1 — Amplitude-speed relationship. Displayed are sample data from several theories that claim high accuracy. The numerical results of previous investigators generally fall below those obtained by other means, except for the highest wave. Our calculations of the relationship data agree with those of Longuet-Higgins and Fenton (1974) and with Byatt-Smith and Longuet-Higgins (1976), except for very high waves.

Manuscript submitted on June 24, 1981.

*This fact has been known since Stokes (see Lamb, 1932 Art. 250), if not before; it is the result of the highest wave's possessing a sharp crest, i.e., a discontinuous slope. The only way that this can occur is if the fluid at the crest moves at the same speed as the wave itself. The Bernoulli Law then demands the limiting-height-speed relationship.

Methods used to deduce the properties of solitary waves fall into three classes: (a) expansions about a small parameter, e.g. the amplitude, (b) numerical methods, and (c) others. No matter what the method, reliance on numerical computation is necessary to approach the higher waves. Figure 1 presents the results of our calculation, and displays sample results from each of the three methods whose authors claim 4 to 5 figure accuracy. Prior to this work, mutual agreement of the stated accuracies could be found only between the results of Longuet-Higgins and Fenton (1974) and those of Byatt-Smith and Longuet-Higgins (1976). Except for the highest wave, the numerical methods produced somewhat smaller speeds for a given amplitude than did the others. All previous works claiming high accuracy give a limiting wave height within 0.0015 of 0.8270.

Figure 1 shows that for all but the very highest waves, perfect (to the resolution of the figure) agreement is found between the numerical method presented here (the line), and the results of Longuet-Higgins and Fenton (1974) and of Byatt-Smith and Longuet-Higgins (1976). The dilemma remains, however, that the method described here also yields a highest wave higher than previously reported. We feel that a detailed description of our numerical method is called for to discuss why our method gives more accurate results than other numerical methods (Miles, 1980 reviews the status of solitary wave research and points out the unsatisfactory status of knowledge of high solitary waves).

This report is organized as follows: Section 2 develops the basic theory for describing a solitary wave and defines certain conformal transformations that are useful for numerical calculations. Section 3 describes the representation of the solution and identifies features of the solitary wave which are computed. Section 4 describes the numerical procedures used in obtaining solutions. Section 5 compares the results to those of earlier investigators. Section 6 briefly summarizes the results and offers conclusions.

2. BASIC THEORY AND USEFUL TRANSFORMATIONS

A. The Kind of Solitary Wave Considered

Figure 2a shows an idealization of solitary waves in water. Apart from dissipative effects, the wave propagates at a constant speed and without change of form over an impermeable and horizontal bottom. The conventional mathematical model describing the solitary wave takes the fluid to be incompressible and inviscid, with all fluid motions irrotational. In addition, the conventional model neglects surface stresses imposed by the relatively undense air, and imposes a constant pressure boundary condition at the air-water interface. Because only pressure gradients appear in the equations of motion, the upper surface of the water is considered stress-free. The model contemplates only plane waves, so that motion is confined to the x-y plane (see Fig. 2a). By assuming at the start that the wave moves at constant speed and shape through still water, one may make a Galilean transformation to *wave coordinates* where the wave is stationary. Viewed from wave coordinates the situation is then one of a steady, incompressible, irrotational flow in two dimensions.

Two equations completely govern the local motion in the interior of the fluid. These are that $\operatorname{div} \mathbf{u} = 0$ (incompressibility) and $(\operatorname{curl} \mathbf{u})_z = 0$ (irrotationality). It follows that a velocity potential ϕ and a stream function ψ are tied to Cauchy-Riemann conditions:

$$u = \partial\phi/\partial x = \partial\psi/\partial y,$$

$$v = \partial\phi/\partial y = -\partial\psi/\partial x.$$

As is customary, define a pair of complex variables $z = x + iy$ and $w = \phi + i\psi$. Then the local motion in the interior of the fluid is satisfied by any analytic function $w = w(z)$, or, alternately $z = z(w)$. Figure 2b is the map to w-space.

It remains to pose boundary conditions. These are the following: the flow at the bottom of the channel is horizontal; flows away from the wave are horizontal and shear-free, and the same on each

side of the wave; the pressure along the free surface vanishes. Identifying this upper boundary in advance is possible in w-space (it corresponds to ψ = constant). It is not possible in z-space. Therefore, most researchers since Stokes (1880) have selected w to be the independent variable, then $z = z(w)$ is the desired solution. With this choice of independent variable the boundary conditions are:

$$y = 0 \qquad \text{along } \psi = 0 \tag{2}$$

$$\frac{dz}{dw} \to \frac{1}{U} \qquad \text{as } \phi \to \pm\infty \tag{3}$$

$$gy + \frac{1}{2}/\left|\frac{dz}{dw}\right|^2 = gh + \frac{1}{2}U^2 \qquad \text{along } \psi = \psi_0 \tag{4}$$

where g is the acceleration of gravity, h is the water depth away from the wave, and U is the speed of the wave relative to still water. Like Yamada (1957, 1958), we nondimensionalize in the way that minimizes external parameters appearing in z and w. This is the system $h = U = 1$. Equations (2), (3), and (4) then become:

$$y = 0 \qquad \text{along } \psi = 0 \tag{5}$$

$$\frac{dz}{dw} \to 1 \qquad \text{as } \phi \to \pm\infty \tag{6}$$

$$y + \frac{1}{2}F^2/\left|\frac{dz}{dw}\right|^2 = 1 + \frac{1}{2}F^2 \qquad \text{along } \psi = 1 \tag{7}$$

where $F \equiv U/\sqrt{gh}$ is the Froude Number.

Henceforth in this report, solitary waves are defined to be $z = z(w)$ subject to Eqs. (5), (6), and (7). As Fig 1 shows, there may be more than one solitary wave that corresponds to a given F. This remarkable discovery was made by Longuet-Higgins and Fenton (1974), and has been confirmed by other investigators.

B. A Transformation of the Free Surface to a Unit Circle

For the purposes of performing a trustworthy numerical analysis, we found it desirable to move the domain of the nasty boundary condition, Eq. (7), to the unit circle by a conformal transformation. Levi-Civita (1925) and Yamada (1957, 1958) show how to do this. The transformation

$$\zeta \equiv -\tanh^2 \frac{\pi}{4} w \tag{8}$$

maps the region occupied by the fluid into the interior of the unit circle (see Figs. 1b, 1c).

The flow can be described with a new dependent variable:

$$\Omega \equiv i \ln(dw/dz) \equiv \theta + i\tau. \tag{9}$$

In Eq. (9) θ is the angle of surface inclination and $\tau = \ln q$, where q is the fluid speed $\left|\frac{dw}{dz}\right|$. Referring to Fig. 2c, the boundary conditions are:

$$\theta = 0 \qquad \text{along } 0, \pm I \tag{10}$$

$$\Omega = 0 \qquad \text{at } \pm I \tag{11}$$

$$q^2 \frac{dq}{d\sigma} \cos\frac{1}{2}\sigma = \frac{1}{\pi F^2} \sin\theta \qquad \text{on the unit circle.} \tag{12}$$

The last condition is not self-evident (Yamada 1958 gives a derivation). Its integral forms an alternative to Eq. (12):

$$q^3(\sigma) = q^3(0) + \frac{3}{\pi F^2}\int_0^\sigma \sin\theta \sec\frac{1}{2}\sigma\, d\sigma \text{ on the unit circle.} \tag{13}$$

C. Another Useful Transformation

The transformation described in Section 2B of this report has the unfortunate side-effect in which the point marked ± 1 in Fig. 2c is singular. Although we shall use numerical methods that converge despite the singularity, it is possible to improve the accuracy of some of the "derived" (to be defined later) quantities by expanding about the point -1. The independent variable μ is formed by the transformation:

$$\mu \equiv e^{+\beta w} \equiv \xi + i\gamma \tag{14}$$

where β, a positive real number, is defined later. Figure 2d shows the mapping from 2b.

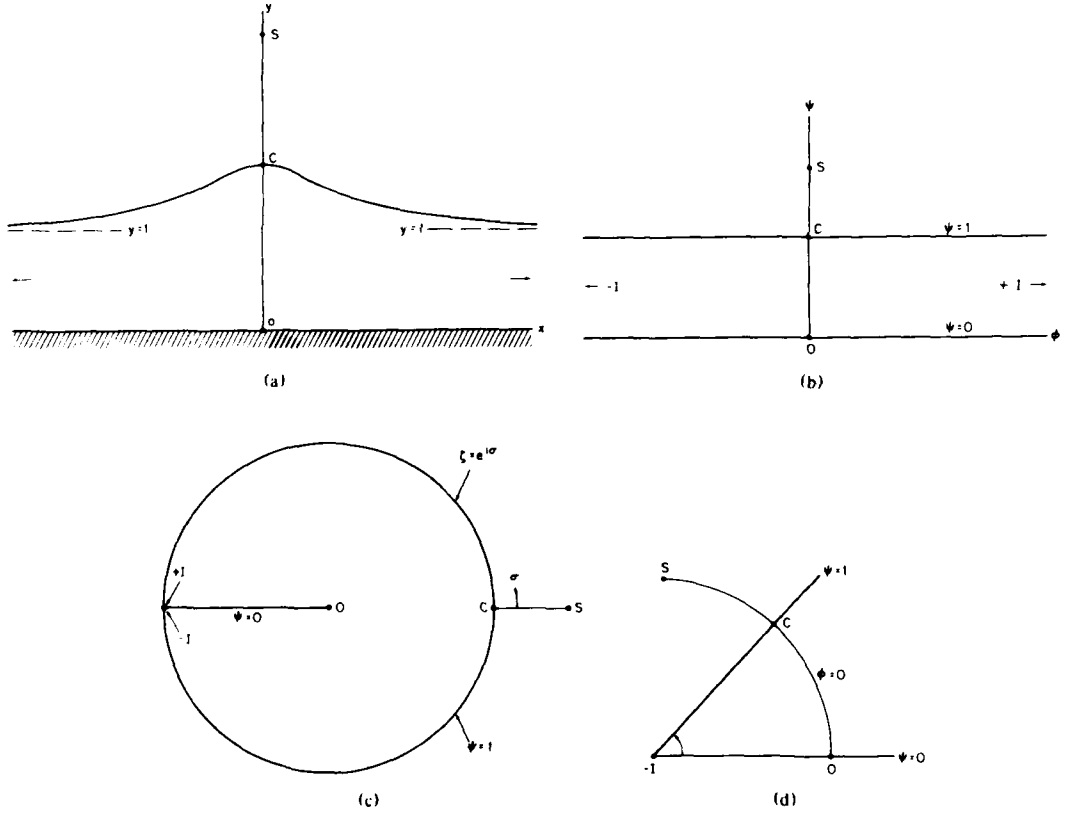

Fig. 2 — Domains of the fluid under various conformal transformations: a. the $z = x + iy$ plane; b. the $w = \phi + i\psi$ plane; c. the mapping of the fluid into the interior of a unit circle; d. the plane appropriate for expansions about a point at infinity. The point marked *S* marks a singularity that can trouble accurate calculations. It is infinitely far away from the fluid in the limit of infinitesimal waves; it approaches the free surface as the wave amplitude approaches its highest value.

In an earlier paper making use of this transformation, Witting (1975) was able to estimate the location and some of the properties of the singularity at S. For the wave of limiting amplitude, the highest wave in water, S is located on the free surface, and its properties are known (see Lamb, 1932 and Grant, 1973).

3. TREATMENT OF THE SINGULARITIES AND DEVELOPMENT OF A FOURIER SERIES SOLUTION

A. Basic Relationships

The aim here is to find a solution for Ω (Eq. (9)) that satisfies the boundary conditions (Eqs. (10), (11), and (13)). We split the solution into two parts, one of which is an attempt to explicitly account for some of the singular behavior at S. Thus,

$$\Omega(\zeta) = \Omega_0(\zeta) + \Omega_r(\zeta) \tag{15}$$

$$\Omega_0(\zeta) = \theta_0 + i\tau_0 \tag{16}$$

$$\Omega_r(\zeta) = \theta_r + i\tau_r . \tag{17}$$

We define Ω_0 to be

$$\Omega_0 = \frac{i}{3} \ln \frac{1 - \lambda\zeta}{1 + \lambda}, \tag{18}$$

where λ is a constant to be defined presently. Note that Eq. (18) satisfies the boundary conditions (Eqs. (10) and (11)), but not necessarily Eq. (13). On the unit circle Eq. (18) gives

$$\sin(3\theta_0) = \frac{\lambda}{1 + \lambda} \frac{\sin\sigma}{q_0^3(\sigma)}, \tag{19}$$

$$q_0(\sigma) = \left[1 - \frac{2\lambda}{(1 + \lambda)^2}(1 + \cos\sigma)\right]^{1/6} \tag{20}$$

and Eqs. (19) and (20) provide the relationship between λ and $q_0(0)$

$$\lambda = \left[1 - q_0^3(0)\right] \left[1 + q_0^3(0)\right]. \tag{21}$$

In the numerical work λ is to be specified, sometimes from specifying q_0 and using Eq. (21). Hence, $\Omega_0(\zeta)$ is determined explicitly. Note that for the highest wave the singular behavior of Ω_0 matches that demanded for a sharp corner along a free surface.

Specifically, when q_0 vanishes, λ is unity, and the singularity in Eq. (18) is on the free surface. Equation (18) goes to:

$$\sigma_0(\sigma) = \frac{\pi - \sigma}{6} \qquad \text{for } 0 < \sigma \leqslant \pi, \tag{22}$$

$$\sigma_0(\sigma) = \frac{-\pi - \sigma}{6} \qquad \text{for } -\pi \leqslant \sigma < 0, \tag{23}$$

$$\tau_0(\sigma) = \frac{1}{3} \ln\left|\sin\frac{1}{2}\sigma\right| .$$

This conforms with the requirement that the total interior angle of the flow is 120°, for

$$\lim_{\sigma \to 0^+} \theta(\sigma) = \frac{\pi}{6} \quad \text{and} \quad \lim_{\sigma \to 0^-} \theta(\sigma) = -\frac{\pi}{6}.$$

As q_0 departs from zero the singularity in Eq. (21) moves away from the free surface, to infinity when $q_0 = 1$. The location of the singularity generally conforms to the estimated locations found by Witting (1975); the nature of the singularity conforms only for the highest wave, but should not be in too much error for almost highest waves. In any case, Ω_0 should account for much of the singular behavior of Ω at S for high waves.

The remaining part of the solution, Ω_r, is represented as the Fourier series:

$$\Omega_r \equiv i \sum_{n=0}^{\infty} a_n \zeta^n. \tag{24}$$

The boundary condition Eq. (10) demands that all a_n be real.

The components of Ω_r on the free surface are:

$$\theta_r(\sigma) = -\sum_{n=1}^{\infty} a_n \sin n\sigma \tag{25}$$

and

$$\tau_r(\sigma) = \sum_{n=0}^{\infty} a_n \cos n\sigma. \tag{26}$$

These are the (real) Fourier expansions of θ_r and τ_r; knowledge of either as a function of σ permits the calculation of a_n through various techniques; we use the fast Fourier transform.

Specifically, Eq. (13) is the governing equation used to calculate the a_n. Only the interval $(0,\pi)$ is needed. The final boundary condition, 11, is that $q(\pi) = 1$. Hence, Eq. (13) has the extra information that:

$$1 = q^3(0) + \frac{3}{\pi F^2} \int_0^{\pi} \sin\theta \sec\frac{\sigma}{2}\, d\sigma, \tag{27}$$

which relates F^2 to $q(0)$ and $\theta(\sigma)$.

Bernoulli's Law gives the amplitude:

$$\alpha = \frac{1}{2} F^2[1 - q^2(0)], \tag{28}$$

and by quadrature it is an easy matter to compute a profile using the relationship

$$dx + i dy = -\frac{1}{\pi} \frac{e^{i\theta(\sigma)}}{q(\sigma)} \sec\frac{\sigma}{2}\, d\sigma \tag{29}$$

that arises from Eqs. (8) and (9) once θ and q are known.

A final check may be made to test for gross programming or other errors. The test is to see whether the pressure, initially set to zero by Eq. (7) is actually zero at the end. This (kinematic) pressure p is:

$$p = \frac{1}{2}(1 - q^2) - \frac{1}{F^2}(y - 1). \tag{30}$$

Obviously, that p defined above be small is a necessary condition for an accurate solution; however, it is not a sufficient condition, as we shall see later.

B. Derived Relationships

The parameter $q(0)$ is the input parameter that serves to distinguish one solitary wave from another. We call those other parameters *basic* that arise most directly from the calculations and are

computed to the highest precision. These are F^2, α, q, and θ. *Derived* parameters are those that come less directly from the calculations, or cannot be computed with the highest precision. The first of these were given in Eq. (29), namely the horizontal and vertical coordinates, from which a profile can be generated.

Other derived quantities of interest are defined below. The solitary wave mass M is:

$$M = \int_{-\infty}^{\infty} \eta \, dx, \tag{31}$$

where η is the elevation above still water level. A parameter closely related to the potential energy is

$$V \equiv \frac{1}{2} \int_{-\infty}^{\infty} \eta^2 dx. \tag{32}$$

Three parameters are of interest at the flanks of the solitary wave. An expansion in powers of μ (see Eq. (14)) leads to a surface profile specified by:

$$x = \phi - x_0 + a_1 e^{\beta\phi} \cos\beta + O(e^{2\beta\phi}) \tag{33}$$

$$\eta = a_1 e^{\beta\phi} \sin\beta + O(e^{2\beta\phi}) \qquad \text{as } \theta \to -\infty. \tag{34}$$

In Eqs. (33) and (34) β satisfies

$$F^2 = \frac{\tan\beta}{\beta}; \quad \beta < \pi/2. \tag{35}$$

The three parameters of interest are β, x_0, and a_1, or alternatively, B, defined by:

$$\eta \to Be^{-\beta|x|} \quad \text{as } |x| \to \infty. \tag{36}$$

The horizontal drift $2x_0$ is identically the circulation C in the nondimensionalization used here. Knowledge of M or V, and C is sufficient to determine other integral properties of interest, using the relations given by Longuet-Higgins (1974). Once profiles have been computed, it is easy to compute x_0, B, and either M or V or both.

4. DEVELOPMENT OF NUMERICAL SOLUTIONS

A. The Solution at a Fixed Resolution

Except for our explicit treatment of the singularity at S with the function Ω_0, our procedure is similar to that of Yamada (1957, 1958). Table 1 gives a partial description of the steps required in forming a basic iterative solution at a given resolution, i.e., value of N. First, a value for $q(0)$ is specified. This identifies a unique wave. The auxiliary function Ω_0 is chosen so that $q_0(0) = q(0)$, which determines λ. A total of $N + 1$ Fourier coefficients a_n form a solution. There are N subdivisions in the interval $0 < \sigma < \pi$. Thus, quantities that are functions of σ are determined at points $\sigma_n = n\pi/N$ with $n = 0, 1, 2, \ldots, N$. At the start we let all the a_n's be zero.

Steps 5 to 13 of Table 1 outline the iterative procedure. From our experience the most delicate aspect of the procedure occurs at Step 7, because the integral appearing in Eq. (27) is singular at $\sigma = \pi$. It is possible to show that θ has a vertical asymptote at $\sigma = \pi$ but that the singularity is integrable (we find no reference to these facts in earlier work). A simple approach is to ignore the singularity and evaluate the integrand at the endpoint by using the limit

$$\lim_{\sigma \to \pi} \sin\theta \sec\frac{1}{2}\sigma = -2\theta'(\pi) \tag{37}$$

where the prime denotes the first derivative. We adopt this simple approach. Even though the singularity is not treated elegantly, the error should be small for N sufficiently large. We tried to develop methods to improve our treatment of this singularity, but without success.

Table 1 — The Numerical Recipe

Step Number	Step	Equation(s) and Methods Used
1	Choose $q(0)$, N	
2	Set $q_0(0) = q(0)$	
3	Compute $\Omega_0(\zeta) \equiv \theta_0(\zeta) + i\tau_0(\zeta)$	18,21
4	Set $a_n = 0$ for all n. This completes initialization.	
5	Compute $\theta_r(\sigma)$	25
6	Compute $\theta = \theta_0 + \theta_r$	
7	Obtain F^2	27, Simpson's Rule
8	Compute α	28
9	Test to see whether α has changed significantly from the previous iteration. If not, this is the final iteration.	
10	Compute $q(\sigma)$	13
11	Compute $\tau_r(\sigma) = \ln q(\sigma) - \tau_0(\sigma)$	
12	Compute a new set of a_n's	26, Fast Fourier Transform
13	Return to step 5 if this is not the final iteration. Continue if it is the final one.	
14	Compute θ, q, the profile, and other derived quantities.	

Rather than specify $q(0)$, one can just as well specify the quantity ω defined by

$$\omega \equiv 1 - F^2 q^2(0). \tag{38}$$

This produces some slight modifications to Table 1. We use the modified procedure to produce results that can be compared to those of Longuet-Higgins and Fenton (1974) and Byatt-Smith and Longuet-Higgins (1976).

The test used to stop the iteration process is that successive values of α differ by less than 10^{-6}. Up to 40 iterations are required. An example of the convergence process is shown in Table 2. The results display features found in every case examined: (a) The higher resolution samples (large N) start much closer to their final value than do the coarser resolution samples. (b) The coarse resolution samples are more rapidly convergent. Fewer iterations are usually required for the finer resolution calculations. The slowness of convergence for $N = 1440$ in Table 2 makes it risky to trust the last digit. The limiting amplitudes and speeds differ significantly between one resolution and the other. Why this is so is addressed later.

Table 2 — Convergence of Process to Obtain Solitary Wave Conditions for a Given ω. The value of ω is 0.50.

Iteration Number	$N = 90$		$N = 1440$	
	a/h	F^2	a/h	F^2
1	0.506102	1.512203	0.480272	1.460544
2	0.476858	1.453715	0.480275	1.460549
3	0.465467	1.430933	0.480278	1.460556
4	0.463457	1.426915	0.480283	1.460566
5	0.465758	1.431517	0.480290	1.460579
6	0.469426	1.438852	0.480297	1.460595
7	0.472924	1.445847	0.480306	1.460612
8	0.475618	1.451236	0.480314	1.460628
9	0.477404	1.454809	0.480321	1.460642
10	0.478429	1.456858	0.480327	1.460655
11	0.478917	1.457833	0.480332	1.460664
12	0.479078	1.458155	0.480336	1.460672
13	0.479070	1.458139	0.480339	1.460677
14	0.478995	1.457989	0.480340	1.460681
15	0.478909	1.457818	0.480342	1.460683
16	0.478839	1.457677	0.480342	1.460685
17	0.478790	1.457580		
18	0.478761	1.457523		
19	0.478748	1.457495		
20	0.478743	1.457486		
21	0.478743	1.457486		

As pointed out earlier, a necessary condition for an accurate solution is that the pressure found from Eq. (30) nearly vanishes. Figure 3 displays that pressure, also for $\omega = 0.50$. The computed pressures are indeed small, never exceeding 0.6×10^{-4}, even at the coarse resolution $N = 90$. They are largest near $\sigma = 180°$, the flanks of the solitary wave. A striking feature in Fig. 3 is the oscillation of the pressure, with an alternating sign at every data point except at 146° to 148°. This oscillation is characteristic of all of the calculations; except for isolated points, its period is always 2 grid points, and so is related to the calculations, not to the wave. We ascribe the oscillations to aliasing in the fast Fourier transform algorithm, though it is possible that it is caused by some other numerical artifact. Although we find the oscillations unpleasant to look at, we do not believe that they indicate a serious problem.

Figure 4 displays the behavior of the computed pressure. On a log scale it plots the envelope of pressure curves like that of Fig. 3, for $N = 180$ and $N = 1440$. The curves for $N = 360°$ and for $N = 720$ are nested within the pair shown. The behavior is typical. The computed pressure increases with σ, is always small, and becomes very small as N becomes large.

B. Extrapolation to Infinite N

Let Q be the exact value of any of the basic or derived variables. The numerical procedures described in Section 4A estimate Q by setting some finite N in advance; call this estimate

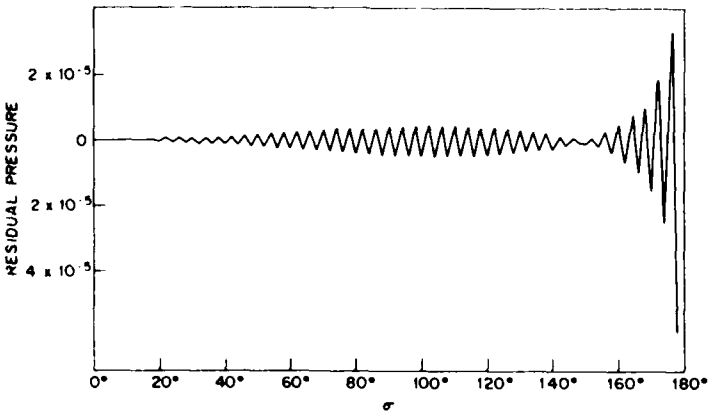

Fig. 3 — Residual pressure for $\omega = 0.50$ from the calculation with $N = 90$. The oscillatory behavior having a period of two grid points is a numerical artifact. It is typical of all our calculations. A node appears near $\sigma = 150°$. Most of the calculations show no node; rather, the magnitude of the residual pressure increases monotonically with σ.

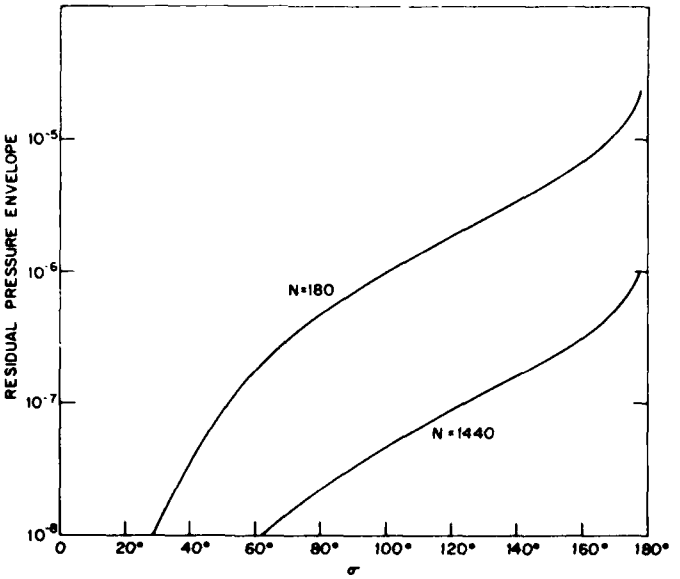

Fig. 4 — Variation of the magnitude of the residual surface pressure along the $\omega = 0.50$ solitary wave. The pressures for the $N = 360$ and $N = 720$ calculations fall between the curves displayed.

Q_N. Presumably, some information about Q should be present in a sequence of Q_N that is absent from any individual Q_N. We guess that a likely behavior is that of a power law, i.e.,

$$Q_N = Q + kN^{-m}, \tag{39}$$

where Q, k, and m are unknown. The calculations are done in multiples of N, specifically, N = 90, 180, 360, 720, and 1440. If Eq. (39) holds exactly, then Q is given by:

$$Q = \frac{Q_{J+1}\,Q_{J-1} - Q_J^2}{Q_{J+1} + Q_{J-1} - 2Q_J^2} \tag{40}$$

(see Shanks, 1955). It turns out that (Eq. 39) appears to be a close approximation, in that the estimates of Q from the triads 360, 720, 1440 and 180, 360, 720 usually are much closer together than Q_{1440} is to either. Moreover, log-log plots of $(Q_N - Q)$ versus (N), which must be straight through the points N = 1440, 720, and 360, also pass through or near the point at N = 180 and usually near the point at N = 90. We believe that extrapolating results gives a closer approximation to the exact value than does the result at the finest resolution (N = 1440).

C. Loss of Accuracy Near the Tails: Connecting the Solution to an Exponential Decay

The use of the fast-Fourier-transform algorithm demands that data be equally spaced, i.e., uniform intervals in σ. As we have seen, this does not produce relatively uniform errors (as measured by the computed pressures) throughout the range of σ. Neither does it reach very far out on the flanks of the solitary wave; values of η_{178° vary between 0.044 (ω = 0.1) to 0.029 (ω = 1.0). For weak waves, this is a substantial fraction of the amplitude. For all waves we match the Fourier transform solution to an exponential falloff at the tails using Eqs. (33) and (34). The solutions are matched at σ = 177° for $N \geqslant 180$.

5. SAMPLE COMPARISONS WITH OTHER WORK

Longuet-Higgins and Fenton (1974), by a method totally different from ours (an expansion method), use ω to specify wave properties. They cite 5-place accuracy in wave speed and amplitude up to ω = 0.75. Through this region (and somewhat beyond, but where comparisons can be made only to 4-place accuracy) near-perfect agreement between their results and ours exists. Figure 1 shows agreement, but does not indicate how remarkable the agreement actually is. We claim about 5-place accuracy from ω = 0.45 to breaking. Figure 5 shows the wave-speed results as a function of N for ω = 0.45 and ω = 0.75 along with the results of Longuet-Higgins and Fenton (1974). These wave strengths lie at the ends of the range where both theories claim about 5-place accuracy (six significant figures in F^2).

It is evident from the figure that the limiting values are close—between 0×10^{-5} and 3×10^{-5}. It is also evident that the extrapolation procedure helps a little when ω = 0.75 and helps greatly when ω = 0.45. This is characteristic. The extrapolated value of all parameters lies closer to the N = 1440 value the closer ω is to unity. The calculations over the range $0 < \omega \leqslant 0.75$ agree with those of Longuet-Higgins and Fenton (1974) for all variables given by them. For ω = 0.80 and above there are small (but mathematically significant) differences in some of the solitary wave parameters (see NRL Report 8505 for details). There our calculations agree more closely with the more recent work of Byatt-Smith and Longuet-Higgins (1976). The detailed comparisons with high solitary waves are deferred to NRL Report 8505.

Given the favorable comparison with work using an independent method, the question remains why the comparison is unfavorable with other numerical methods (see Fig. 1). To provide some insight, we reduced N to resemble the resolution of Yamada (1957, 1958), whose numerical method most closely resembles our own, i.e., he used a Fourier Series method of numerical solution.

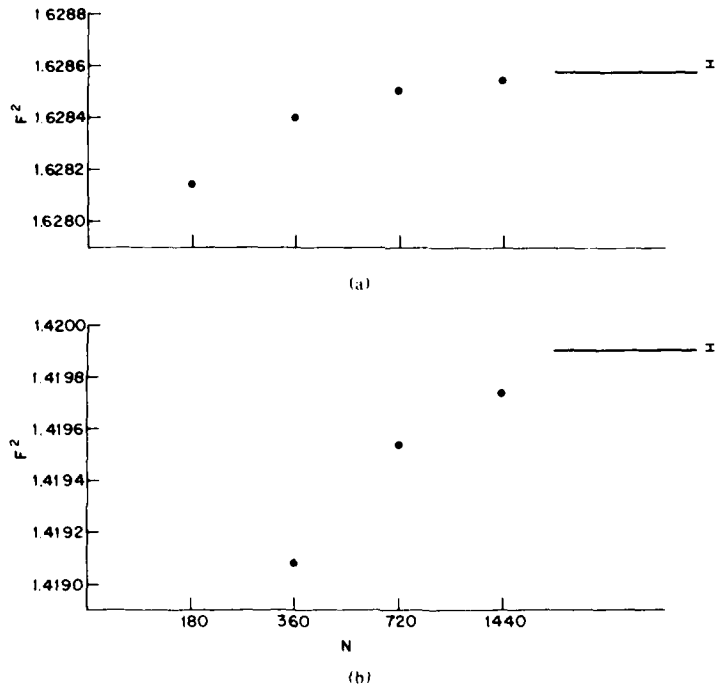

Fig. 5 — Calculation of the wave speed for (a) $\omega = 0.75$ and for (b) $\omega = 0.45$. The points show the speeds resulting from calculations at the various resolutions specified by N. The line is the limiting value from Eq. (40) from estimates at $N = 360$, 720 and 1440. The error bars show the speeds found by Longuet-Higgins and Fenton (1974), who use a totally independent method. They give F to five decimal places; the error bars bracket the range 0.000005 from their stated values.

Specifically, we select $N = 12$, 24, 48, 90, 180, 360, 720, and 1440 for $q(0) = 1/\sqrt{3}$ (Yamada, 1958) and for $q(0) = 0$ (the highest wave; Yamada, 1957). Yamada used $N = 12$, probably the limit for the time. Figure 6 draws the comparison. Yamada's result and ours for $N = 12$ are comparable (his grid system and numerical procedure differed somewhat from ours, however, and the agreement is imperfect). We conclude from the figure that our results are consistent with Yamada's, but that $N = 12$ is insufficient to produce even 2-place accuracy in α or $F^2 - 1$.

Many error estimates of numerical work on the solitary wave problem are based on the smallness of the pressure as an indicator of errors in, say, the amplitude. In the example of Table 2 and Fig. 3, $\omega = 0.50$, the pressure residuals are small, but errors in the speed and amplitude are not so small. Specifically, for $N = 90$ Table 2 indicates an error of 0.0016 in amplitude and 0.0032 in F^2, although the residual surface pressures never exceed 0.00006 and are much smaller over most of the range of σ (Fig. 3).

Figure 7 shows residual pressures and estimated errors in α and F^2 for $\omega = 0.45$. We see that the estimated error exceeds the surface pressure computed at all parts of the wave by two orders of magnitude or more; the excess is greater than three orders of magnitude for a central point ($\sigma = 90°$). In addition, the slope of the estimated error differs somewhat from that of the computed pressures (which themselves are parallel). This means that a simple multiplicative factor is insufficient to relate computed surface pressure to errors in solitary wave properties. We find that residual pressures are always much less than estimated errors in wave speed and amplitude.

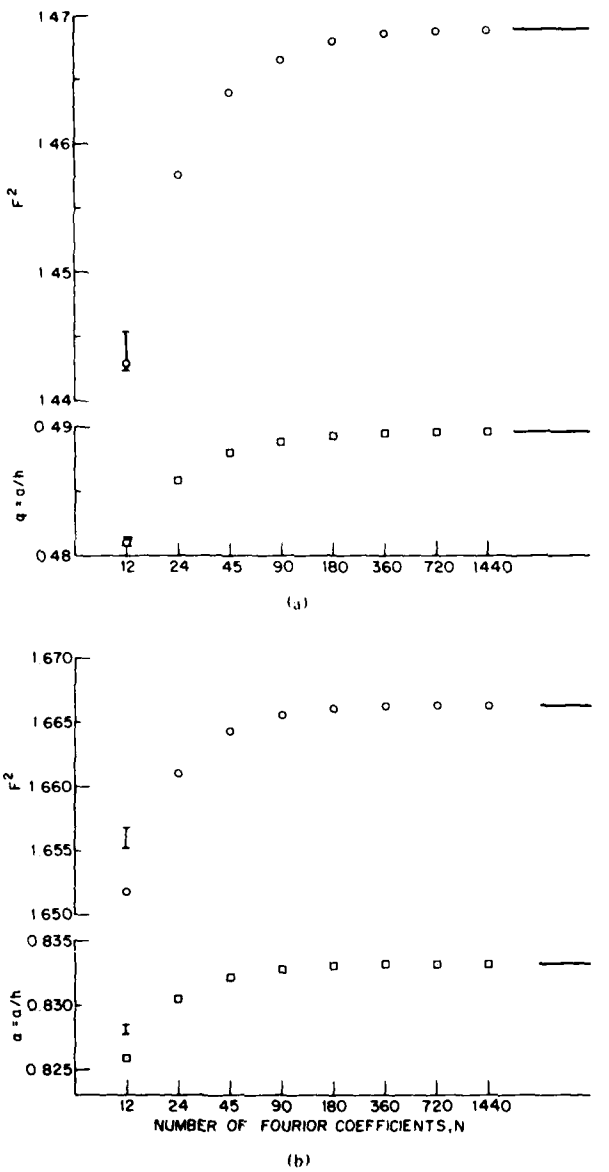

Fig. 6 — Calculation of the wave speed and amplitude for (a) $q(0) = 1/\sqrt{3}$ and for (b) $q(0) = 0$, the highest wave. The open points display the results calculations at the various resolutions specified by N. The line is the limiting value from Eq. (40) from estimates at $N = 360$, 720 and 1440. The error bars show the data from (a) Yamada (1958) and (b) Yamada (1957). Calculations with resolutions around $N = 12$ fail to give solutions accurate to two decimal places in F^2 or a/h.

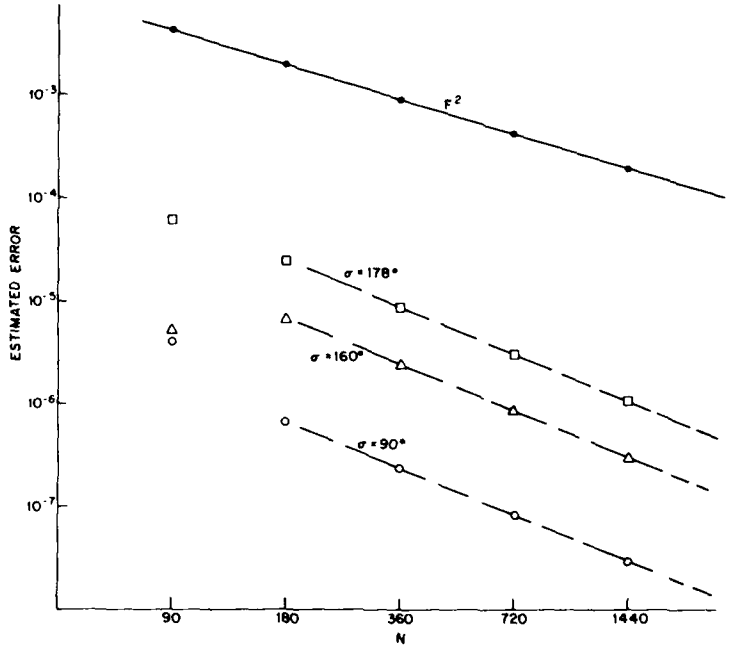

Fig. 7 — Estimated errors for $\omega = 0.45$. The uppermost curve estimates the error in F^2. The error in a/h is one-half of this. The estimate is formed by taking the data at $N = 360$, 720, and 1440 and applying Eq. (40). This ensures that the last three points fall on a straight line; that the first two also fall on the same line indicates that the form of the extrapolation defined by Eq. (40) is a good one. The data shown with open symbols give the residual pressures at particular points on the profile of the solitary wave. It is evident that the residual pressures are poor indicators of the errors in speed and amplitude.

6. SUMMARY AND CONCLUSIONS

We have refined the numerical method developed by Yamada (1957, 1958) to compute the properties of solitary waves. The major refinements are: extending the resolution of the calculations to the limit of our computer, probing into the nature of the behavior of some of the resultant parameters as a function of resolution, and extrapolating to the limit of fine resolution. In addition, an auxiliary function is included to mitigate problems caused by a singularity outside the fluid near the crest. Unlike some more recent work, we went to the Fourier series method of solution for two reasons: (a) the fast Fourier transform algorithm permits computation involving very large numbers of Fourier coefficients, and (b) the properties of Fourier series are well known and favorable. Specifically, the Fourier series is convergent even for functions which are singular at a point on the unit circle.

The agreement with calculations using nonnumerical methods is impressive. Where comparisons of speed or amplitude can be made to five significant figures, there is disagreement by no more than 3×10^{-5}, except for very high waves. There is no reason to suspect that the numerical methods used here deteriorate for very high waves (details are in NRL Report 8505). This is the first numerical treatment of solitary waves which agrees with independent methods to anywhere near the four decimal places usually stated.

What went wrong with the other numerical methods? In the case of Yamada (1958) we have shown that the number of Fourier coefficients used is insufficient to produce highly accurate results. Moreover, the use of surface pressure as an indicator of errors in wave amplitude and speed can be very misleading—by large factors (orders of magnitude). We suspect that the same problems may occur in other numerical treatments, i.e., insufficient resolution and the use of the residual surface pressure to provide an error estimate. In addition, the singularity at $\sigma = 180°$ may cause unrecognized, perhaps-large errors.

REFERENCES

Byatt-Smith, J.G.B. and Longuet-Higgins, M.S., On the speed and profile of steep solitary waves. *Proc. Roy. Soc. London* A **350**, 175-189, 1976.

Grant, M.A., The singularity at the crest of a finite amplitude progressive Stokes wave. *J. Fluid Mech.* **59**, 257-262, 1973.

Lamb, H., *Hydrodynamics.* Cambridge: University Press, 6th ed. (rep. Dover, New York), 1932.

Levi-Civita, T., Determination rigoureuse des ondes permanentes d'ampleur finie. *Math. Ann.* **93**, 264-314, 1925.

Longuet-Higgins, M.S., On the mass, momentum, energy and circulation of a solitary wave. *Proc. Roy. Soc. London* A **337**, 1-13, 1974.

Longuet-Higgins, M.S. and Fenton, J.D., On the mass, momentum, energy and circulation of a solitary wave. II. *Proc. Roy. Soc. London* A **340**, 471-493, 1974.

Miles, J.W., Solitary waves. *Annual Rev. Fluid Mech.* **12**, 11-43, 1980.

Sasaki, K. and Murakami, T., Irrotational, progressive surface gravity waves near the limiting height. *J. Oceanog. Soc. Japan* **29**, 94-105, 1973.

Shanks, D., Non-linear transformations of divergent and slowly convergent sequences. *J. Math. & Phys.* **34**, 1-42, 1955.

Stokes, G.G., Supplement to a paper on the theory of oscillatory waves. *Mathematical and Physical Papers*, Cambridge: Univ. Press pp. 314-326, 1880.

Witting, J., On the highest and other solitary waves. *SIAM J. Appl. Math.* **28**, 700-719, 1975.

Witting, J., High Solitary Waves in Water: Results of Calculations, NRL Report 8505.

Yamada, H., On the highest solitary wave. *Rep. Res. Inst. Appl. Mech. Kyushu Univ.* **5**, 53-67, 1957.

Yamada, H., On approximate expressions of solitary wave. *Rep. Res. Inst. Appl. Mech. Kyushu Univ.* **6**, 35-47, 1958.

Yamada, H., Kimura, G., and Okabe, J., Precise determination of the solitary wave of extreme height on water of a uniform depth. *Rep. Res. Inst. Appl. Mech. Kyushu Univ.* **16**, 15-32, 1968.

END

DATE
FILMED

12-81

DTIC